15

Controlling a Finger-arm Robot to Emulate the Motion of the Human Upper Limb by Regulating Finger Manipulability

Jian HUANG[1], Masayuki HARA[2] and Tetsuro YABUTA[3]
[1]*Kinki University,*
[2]*Swiss Federal Institute of Technology (EPFL),*
[3]*Yokohama National University,*
[1,3]*Japan*
[2]*Swiss*

1. Introduction

The human upper limb possesses a high degree of freedom (DOF) and its redundant structure permits greater flexibility in various dexterous manipulations. The simplest structure of a multifingered robot arm is constructed by fixing a robot finger onto the end effector of a robot arm. A robot with such a structure is also called a macro-micro manipulator (Nagai & Yoshigawa, 1994, 1995; Yoshikawa, et al. 1993). Similar to the human upper limb, the finger-arm robot exhibits a high redundancy. The movement of the robots with such high redundancies creates the problem of how to determine the numerous DOFs of its joints.

Controlling a robot with a high degree of redundancy is a fundamental problem in the field of robotics. A large number of studies have been published on the methodology for determining the redundant DOFs of a robot. Avoidance control of kinematics singularity (Nakamura & Hanafusa, 1986; Furusho & Usui 1989) and obstacle collision avoidance (Khatib, 1986; Maciejewski & Klein, 1985; Loeff & Soni, 1975; Guo & Hsia, 1993; Glass et. Al, 1995) by using redundant DOFs has been mostly investigated. In order to realize desired solutions for the above mentioned problems, methods involving null space (Vannoy & Xiao, 2004) and the criterion function (Kim & Kholsa, 1992; Ma & Nechev, 1995; Ma et al, 1996) have been typically applied.

The finger-arm robot is unlike conventional redundant manipulators. The finger is usually lightweight and has a small link size as compared to the arm. Therefore, it is inappropriate to directly apply the methods developed for controlling a redundant manipulator to the finger-arm robot. To achieve the dexterity like the human hand-arm, a lightweight finger should be actively moved whereas the arm cooperate the movement of the finger, which will greatly improve the performance of a robot (Khatib, 1995; Melchiorri & Salisbury, 1995). The human hand-arm system exhibits similar features. The human hand is obviously lighter, smaller and more sensitive as compared to the arm. The hand-arm coordination is well organized by the central nervous system so as to generate a natural motion. The motivation of this study is to develop a control method emulating a natural movement similar to that of a human upper limb.

Source: Motion Control, Book edited by: Federico Casolo,
ISBN 978-953-7619-55-8, pp. 580, January 2010, INTECH, Croatia, downloaded from SCIYO.COM

Inspired by the human hand-arm movement, a motion control algorithm of a finger-arm robot has been proposed in our study based on the concept of using manipulability of the finger. An effective motion can be generated using the proposed method rather than merely calculating a geometric path for a kinematics solution or optimizing certain dynamic criteria by using the robot's redundant DOFs.

In our study, a heuristic motion control method for a finger-arm robot is firstly proposed. Using the heuristic method, the motion of the arm is heuristically determined by the manipulability of the finger (Huang et al., 2006, Quan et al., 2006). The arm moves to cooperate with the finger's movement in order to maintain finger's manipulability at a desired level. Thus, complicated motions of the finger-arm can be simply divided into separate motions for the arm and for the finger.

However, from the viewpoint of manipulability regulation, the performance of this heuristic method is unsatisfactory, especially when the finger's manipulability is actively required. To improve the property of manipulability regulation, a control of algorithm that employs the steepest ascent method to actively modulate the finger's manipulability is also proposed. Using the steepest ascent method, manipulability of the finger can be immediately increased when it drops below a given reference. As a result, the finger is robust to its singularity. We performed several experiments to demonstrate the effectiveness of the proposed methods.

2. The finger-arm robot and kinematics

2.1 Overview of the system

In this study, a robot finger with three compact motors (Yasukawa Co.) and a robot arm with six DOFs (PA–10, Mitsubishi Heavy Industry Co.) are used as shown in Fig.1. The finger robot is fixed onto the end effector of the robot arm. Such a finger-arm robot has 9 DOFs, whereas a task to be completed in the 3D space of the robot's base coordinate Σ_b requires 6 DOFs. Therefore, three DOFs are redundant. The task to be completed in this study is to generate a motion to trace a desired curve with the fingertip. Since the size of the finger robot is comparatively smaller as compared to that of the manipulator, the finger robot easily reaches its limit.

2.2 Kinematics

The end-effector coordinate and arm base coordinate are set as Σ_t and Σ_b respectively, as shown in Fig.1. The joint angular velocity vector $\dot{\boldsymbol{\theta}} \in R^{9\times1}$ of the finger-arm robot is defined as follows:

$$\dot{\boldsymbol{\theta}} = \begin{bmatrix} \dot{\boldsymbol{\theta}}_a \\ \dot{\boldsymbol{\theta}}_f \end{bmatrix} \tag{1}$$

where $\dot{\boldsymbol{\theta}}_a \in R^{6\times1}$ and $\dot{\boldsymbol{\theta}}_f \in R^{3\times1}$ are the joint angular velocities of the arm and the finger, respectively. Of the arm's end-effector position and orientation $\boldsymbol{p}_t \in R^{6\times1}$ in Σ_b as well as of the fingertip position and orientation $\boldsymbol{p}_f \in R^{6\times1}$ in Σ_b are defined as follows:

$$\boldsymbol{p}_t = \begin{bmatrix} x_t & y_t & z_t & \alpha_t & \beta_t & \gamma_t \end{bmatrix}^T \tag{2}$$

$$\boldsymbol{p}_f = \begin{bmatrix} x_f & y_f & z_f & \alpha_f & \beta_f & \gamma_f \end{bmatrix}^T \tag{3}$$

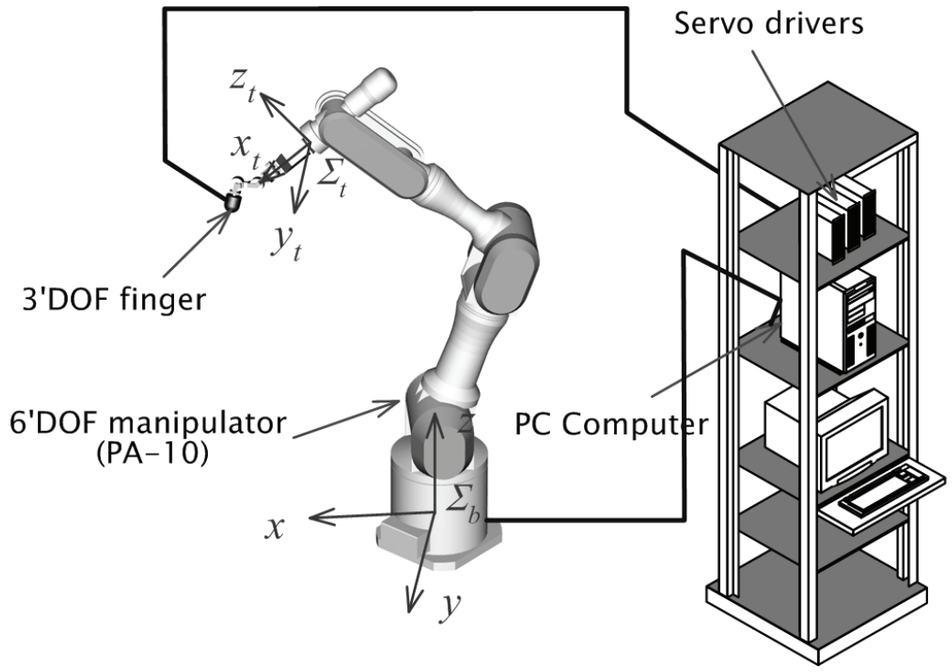

Fig. 1. Schematic diagram of the finger-arm robot

The relationship between its joint angular velocity $\dot{\boldsymbol{\theta}}$ and the fingertip velocity $\dot{\boldsymbol{p}}_f$ in Σ_b can be theoretically expressed as follows:

$$\dot{\boldsymbol{p}}_f = \boldsymbol{J} \cdot \dot{\boldsymbol{\theta}} \tag{4}$$

where $\boldsymbol{J} \in R^{6\times 9}$ is the Jacobian of the finger-arm robot. For the robot arm, we have

$$\dot{\boldsymbol{p}}_t = \boldsymbol{J}_a \cdot \dot{\boldsymbol{\theta}}_a \tag{5}$$

where $\boldsymbol{J}_a \in R^{6\times 6}$ is the Jacobian of the arm. For the finger, it is known that

$${}^t\dot{\boldsymbol{p}}_f = \boldsymbol{J}_f \cdot \dot{\boldsymbol{\theta}}_f \tag{6}$$

where $\boldsymbol{J}_f \in R^{3\times 3}$ is the Jacobian of the finger, and ${}^t\dot{\boldsymbol{p}}_f \in R^{3\times 1}$ is the fingertip velocity in coordinates Σ_t.
If a non-redundant robot is used, the Jacobian $\boldsymbol{J}$ is invertible. Subsequently, the joint angular velocity can be obtained as follows:

$$\dot{\boldsymbol{\theta}} = \boldsymbol{J}^{-1} \cdot \dot{\boldsymbol{p}} \tag{7}$$

However, because a redundant robot is used in our study, the Jacobian $\boldsymbol{J}$ in (4) is not a square matrix. Therefore, its inverse $\boldsymbol{J}^{-1}$ cannot be computed.

2.3 Manipulability of the finger

In robotics, manipulability is used as a criterion to describe the moving potential of a robot (Yoshikawa, 1985). Here, the manipulability W_f of the finger in Fig.1 is calculated as follows

$$W_f = \sqrt{\det(\boldsymbol{J}_f(\boldsymbol{\theta}_f)\cdot \boldsymbol{J}_f^T(\boldsymbol{\theta}_f))} \\ == l_2 l_3 \sin\theta_3 \left(l_1 + l_2 \sin\theta_2 + l_3 \sin(\theta_2+\theta_3)\right) \tag{8}$$

where $\boldsymbol{J}_f \in R^{3\times3}$ is the Jacobian of the finger, and the vector $\boldsymbol{\theta}_f = \begin{bmatrix}\theta_1 & \theta_2 & \theta_3\end{bmatrix}^T$ denotes the joint angles of the finger, l_i (i=1, 2, 3) is the i^{th} link length of the finger.
When a human being requires his fingers and arm to perform a task, his limb is maneuvered such that his hand covers the largest possible range and the task is easily completed. In robotics, this property of the moving potential is referred to as manipulability.

3. Methods of motion control

3.1 The Heuristic Method (HM)

We assume T is the control cycle. As shown in Fig.2, at time t=kT, (k=0, 1, 2, ⋯) the fingertip moves along a desired trajectory $\boldsymbol{p}_d(k) \in R^{3\times1}$ in the arm's base coordinates Σ_b.

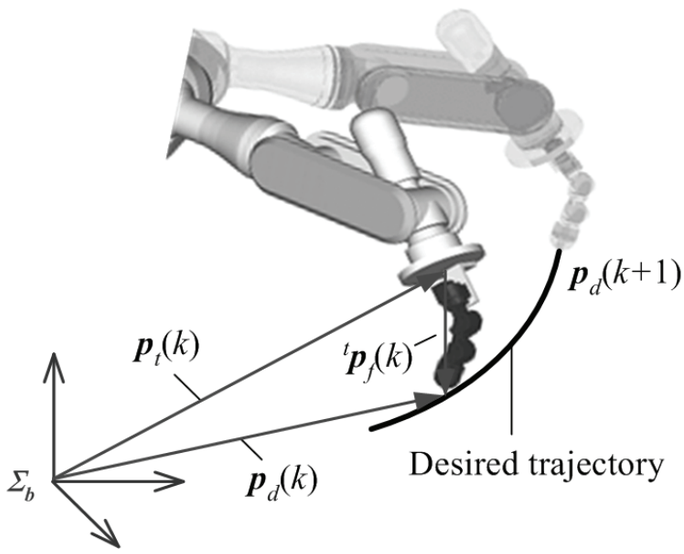

Fig. 2. Position vectors of the finger and the arm

The position of the arm's end-effector in Σ_b is $\boldsymbol{p}_t(k)$ and the fingertip position in Σ_t is ${}^t\boldsymbol{p}_f(k)$. Thus, we have

$$\boldsymbol{p}_d(k) = \boldsymbol{s}_1 \boldsymbol{p}_t(k) + \boldsymbol{R}_t \cdot {}^t\boldsymbol{p}_f(k) \tag{9}$$

where $\boldsymbol{R}_t \in R^{3\times3}$ is the rotation matrix of the arm in Σ_b, and $\boldsymbol{s}_1 \in R^{3\times6}$ is a constant matrix given as follows:

$$\boldsymbol{s}_1 = \begin{bmatrix} 1 & 0 & 0 & 0 & 0 & 0 \\ 0 & 1 & 0 & 0 & 0 & 0 \\ 0 & 0 & 1 & 0 & 0 & 0 \end{bmatrix} \tag{10}$$

If we assume that the orientation of the arm remains unchanged, the rotation matrix $\boldsymbol{R}$ is a constant. Thus, from (9), we get

$$\Delta \boldsymbol{p}_d(k) = \boldsymbol{s}_1 \Delta \boldsymbol{p}_t(k) + \boldsymbol{R}_t \cdot \Delta^t \boldsymbol{p}_f(k) \tag{11}$$

Where

$$\begin{aligned} \Delta \boldsymbol{p}_d(k) &= \boldsymbol{p}_d(k) - \boldsymbol{p}_d(k-1) \\ \Delta \boldsymbol{p}_t(k) &= \boldsymbol{p}_t(k) - \boldsymbol{p}_t(k-1) \\ \Delta^t \boldsymbol{p}_f(k) &= {}^t\boldsymbol{p}_f(k) - {}^t\boldsymbol{p}_f(k-1) \end{aligned} \tag{12}$$

Using (6), (11) can be expressed as

$$\begin{aligned} \Delta \boldsymbol{p}_d(k) &= \boldsymbol{s}_1 \Delta \boldsymbol{p}_t(k) + \boldsymbol{R}_t T \cdot {}^t\dot{\boldsymbol{p}}_f(k) \\ &= \boldsymbol{s}_1 \Delta \boldsymbol{p}_t(k) + T\boldsymbol{R}_t \boldsymbol{J}_f \dot{\boldsymbol{\theta}}_f(k) \end{aligned} \tag{13}$$

When the manipulability W_f is higher than a given reference manipulability W_{fr}, the movement of the arm is unnecessary. According to (13), we have

$$\Delta \boldsymbol{p}_t(k) = 0 \tag{14}$$

Subsequently, we get

$$\Delta \boldsymbol{p}_d(k) = T\boldsymbol{R}_t \boldsymbol{J}_f \dot{\boldsymbol{\theta}}_f(k) \tag{15}$$

Equation (15) expresses that only the finger moves with a joint angular velocity $\dot{\boldsymbol{\theta}}_f$ to trace the desired trajectory. Changing the joint angles of the finger results in a change in $\boldsymbol{J}_f$. As a result, two possibilities of W_f can be considered.

1. If W_f is still higher than W_{fr}, the finger will keep moving and tracing the desired trajectory, while the arm maintains its previous position.
2. If W_f falls below W_{fr}, moving the arm becomes necessary.

Further, if $\Delta \boldsymbol{p}_d(k)$ is theoretically assumed to be completed only by moving the arm, then from (13), we get

$$\Delta \boldsymbol{p}_d(k) = \boldsymbol{s}_1 \Delta \boldsymbol{p}_t(k), \qquad W_f(k) < W_{fr} \tag{16}$$

Thus,

$$\dot{\boldsymbol{\theta}}_f(k) = 0 \tag{17}$$

Equation (17) indicates that the finger stops moving. Hence, the manipulability W_f will remain unchanged as follows:

$$\Delta \boldsymbol{W}_f = 0 \tag{18}$$

Based on (16), we can say that moving the arm instead of moving the finger can theoretically prevent any further decrease in W_f. However, switching control between the arm and the finger by (15)~(17) result in an instant change in velocity.

In this study, in order to achieve the smooth movement of the arm, a desired position $\boldsymbol{p}_{td}(k)$ of the arm at time $t=kT$ is generated by

$$\boldsymbol{p}_{td}(k) = \boldsymbol{p}_t(k-1) + \Delta \boldsymbol{p}_{td}(k) \tag{19}$$

where

$$\Delta \boldsymbol{p}_{td}(k) = A(W_f)\boldsymbol{s}_1^T \Delta \vec{\boldsymbol{p}}_d(k) \tag{20}$$

Here, $A(W_f)$ is a scalar parameter related to the manipulability of the finger. $\Delta \vec{\boldsymbol{p}}_d(k)$ is an unit motion vector in the direction of the desired trajectory and can be computed as follows:

$$\Delta \vec{\boldsymbol{p}}_d(k) = \Delta \boldsymbol{p}_d(k) / |\Delta \boldsymbol{p}_d(k)| \tag{21}$$

In order to move the arm without suddenly changing its velocity, the parameter $A(W_f)$ is heuristically determined by

$$A(W_f) = \begin{cases} 0 & W_f(k) \geq W_{fr} \\ K_a(W_{fr} - W_f(k)) & W_f(k) < W_{fr} \end{cases} \tag{22}$$

where K_a is a selected coefficient.
Compared to (16), the heuristic method shown in (22) yields a smooth motion profile such that the arm moves without any instant change in velocity. Therefore, the finger can also move smoothly. Furthermore, when the generated movement of the arm given in (19) and (20) is larger than the necessary change $\Delta \boldsymbol{p}_d(k)$ of the desired trajectory given by (16), i.e.

$$|\boldsymbol{s}_1 \Delta \boldsymbol{p}_{td}(k)| > |\Delta \boldsymbol{p}_d(k)| \tag{23}$$

the finger will move in a direction such that the manipulability W_f increases. Therefore, we have

$$\Delta W_f \geq 0 \tag{24}$$

In reality, the arm will either not move or move very slowly when $\Delta W_f = W_f - W_{fr}$ is very small because of the friction it experiences at the joint motors and gears. This implies that W_f will probably keep decreasing for a short period. However, further drop of W_f will be definitely prevented as an integral effectiveness with the assist movement of the arm.
The proposed control block diagram of the heuristic method is shown in Fig.3 where, $\boldsymbol{\Lambda}_f$ represents the kinematics of the finger; $\boldsymbol{\Lambda}_a$, the kinematics of the arm; $\boldsymbol{J}_a$, the Jacobian of the arm; $\dot{\boldsymbol{\theta}}_a \in R^{6\times 1}$, the joint velocity of the arm; and $\boldsymbol{G}_f(z)$ and $\boldsymbol{G}_a(z)$, the PID controllers of the finger and the arm, respectively. $\boldsymbol{G}_f(z)$ is defined as:

$$\boldsymbol{G}_f(z) = \boldsymbol{K}_P^f + \boldsymbol{K}_I^f \frac{z}{z-1} + \boldsymbol{K}_D^f (1 - z^{-1}) \tag{25}$$

where $\boldsymbol{K}_P^f \in R^{3\times 3}$, $\boldsymbol{K}_I^f \in R^{3\times 3}$ and $\boldsymbol{K}_D^f \in R^{3\times 3}$ are the given gains of the PID controller. $\boldsymbol{G}_a(z)$ is given as follows:

$$\boldsymbol{G}_f(z) = \boldsymbol{K}_P^f + \boldsymbol{K}_I^f \frac{z}{z-1} + \boldsymbol{K}_D^f (1 - z^{-1}) \tag{26}$$

where $\boldsymbol{K}_P^a \in R^{6\times 6}$, $\boldsymbol{K}_I^a \in R^{6\times 6}$ and $\boldsymbol{K}_D^a \in R^{6\times 6}$ are the given gains of the PID controller.
As shown in Fig.3, when time $t=kT$, based on the finger's manipulability W_f given by (8), the desired position $\boldsymbol{p}_{td}(k)$ of the end-effector of the arm is calculated from (19)~(22).

Subsequently, the desired position ${}^t\boldsymbol{p}_{fd}(k)$ of the finger can be computed by using (9). The obtained $\boldsymbol{p}_{td}(k)$ and ${}^t\boldsymbol{p}_{fd}(k)$are fed as input to each servo loop so as to generate the expected motion.

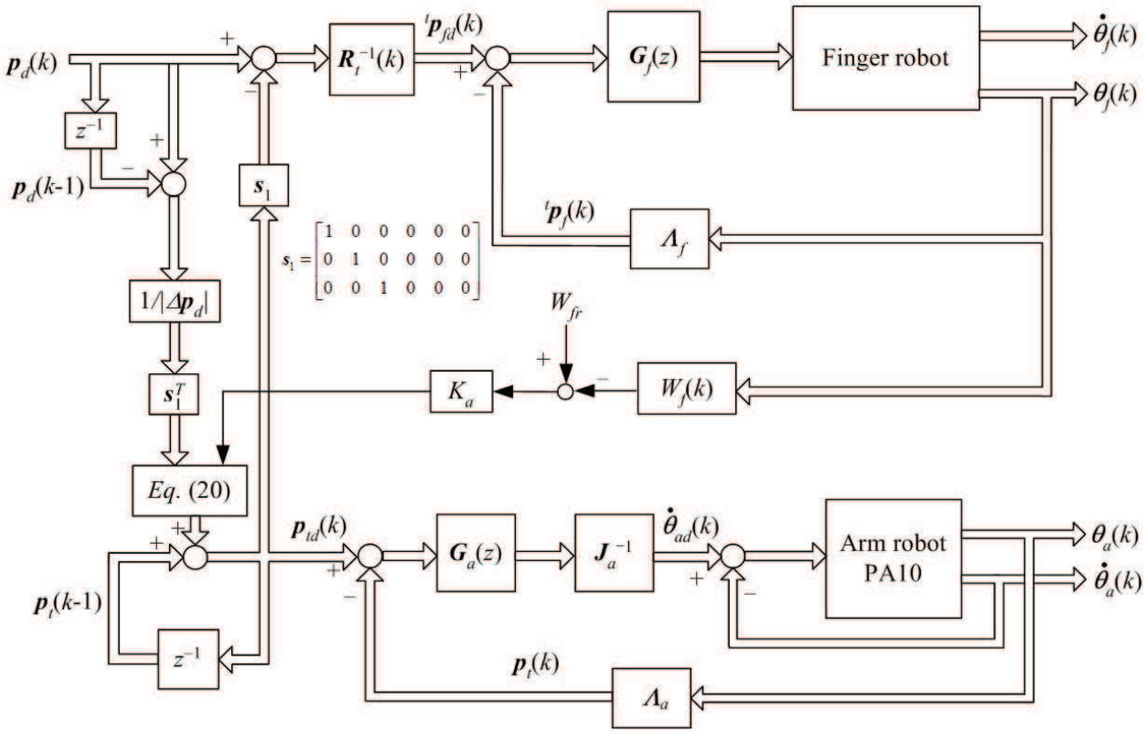

Fig. 3. Control block diagram of the heuristic method

3.2 The Steepest Ascent Method (SAM)

As described above, the basic concept of the heuristic method is to cooperatively move the arm to an expected position by using (19)~(22). The disadvantage of the heuristic method is that the finger's manipulability can not be directly increased. Therefore, it is inappropriate to apply the heuristic method to a task wherein the active modulation of the manipulability of the finger is strongly required. In order to effectively regulate the manipulability of the finger, employing a steepest ascent method is also attempted in our study. The most important feature of this method is that the manipulability of the finger W_f will increase rapidly once it is smaller than the reference value W_{fr}. The details of the algorithm are provided below.

When W_f is higher than W_{fr}, which is similar to the heuristic method, the movement of the arm is unnecessary. Therefore, only the finger moves to trace the desired trajectory as (15)

Whenever the manipulability of the finger reduces to a level smaller than the given reference W_{fr}, the movement of the arm is triggered. At this time, we apply the steepest ascent method to modulate the manipulability W_f of the finger by

$$\boldsymbol{\theta}_{fd}(k) = \boldsymbol{\theta}_{fd}(k-1) + \lambda \frac{\partial W_f}{\partial \boldsymbol{\theta}_f} \tag{27}$$

where λ is the gain coefficient. According to (8), for the finger robot, we have

$$\begin{cases} \dfrac{\partial W_f}{\partial \theta_1} = 0 \\ \dfrac{\partial W_f}{\partial \theta_2} = l_2 l_3 \sin\theta_3 \left(l_2 \cos\theta_2 + l_3 \cos(\theta_2 + \theta_3) \right) \\ \dfrac{\partial W_f}{\partial \theta_3} = l_2 l_3 \left(l_1 \cos\theta_3 + l_2 \cos\theta_3 \sin\theta_2 + l_3 \sin(\theta_2 + 2\theta_3) \right) \end{cases} \tag{28}$$

Then, the fingertip position ${}^t\boldsymbol{p}_f(k)$ in the arm's end effector coordinates Σ_t can be computed from the kinematics expressed as

$${}^t\boldsymbol{p}_f(k) = \Lambda_f(\boldsymbol{\theta}) \tag{29}$$

where $\boldsymbol{\Lambda}_f$ represents the kinematics of the finger robot. Therefore, the desired position $\boldsymbol{p}_{td}(k)$ of the arm's end effector in Σ_b can be computed by

$$\boldsymbol{p}_{td}(k) = \boldsymbol{s}_1^T (\boldsymbol{p}_d(k) - \boldsymbol{R}_t \cdot {}^t\boldsymbol{p}_f(k)) \,. \tag{30}$$

Equations (27)~(30) expresses the arm movement that must be performed once W_f decreases below W_{fr}. To achieve this effect, the arm must move to the desired position specified by (30). Therefore, the finger's joint angle is primarily maintained by the steepest ascent method. As compared to the heuristic method, the manipulability of the finger robot will increase immediately by using the steepest ascent method once it reduces to a level smaller

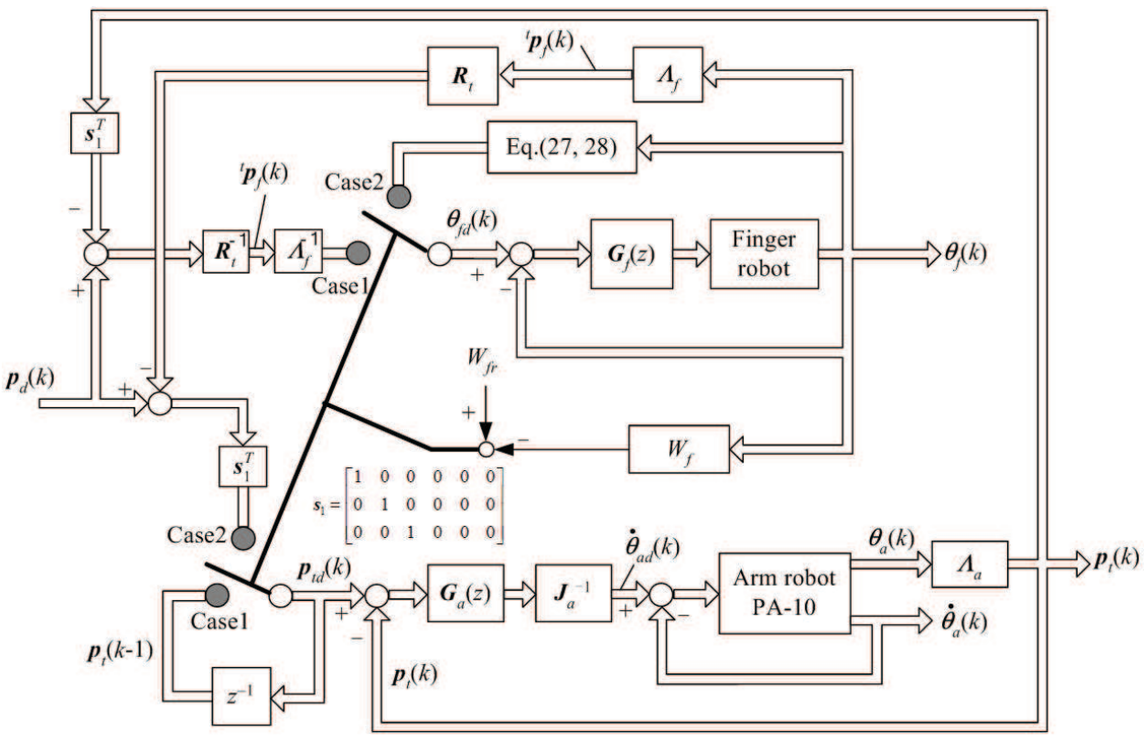

Fig. 4. Control block diagram of applying the steepest ascent method
(Case 1: $W_f > W_{fr}$, Case 2: $W_f \geq W_{fr}$)

than W_{fr}. Moreover, in this study, the steepest ascent method given by (27)~(30) will be applied once it is triggered, and it will be performed until the finger's manipulability reaches an upper threshold W_{ft}. The proposed control block diagram of the steepest ascent method is shown in Fig. 4.

4. Experimental results

To demonstrate the effectiveness of the proposed methods, some experiments were made.

4.1 Motion control using HM

Two distinct desired trajectories are charted out. Since the orientation of the fingertip with respect to the given curve is not specified in the experiment, the orientation of the arm's end-effector is determined as a constant vector. The other related control parameters are listed in Table I.

Control sampling interval, T = 0.005 s, Reference manipulability, W_{fr} = 0.00018,
Control parameters of the arm robot: Initial orientation of the fingertip in Σ_b: a_0 = 0 [rad], β_0 = 1.047 [rad], γ_0 = 0 [rad],
Control parameters of the arm robot: $\boldsymbol{K}_P^a = \mathrm{diag}[5.0 \quad 5.0 \quad 5.0 \quad 2.0 \quad 2.0 \quad 2.0]$ [1/s], $\boldsymbol{K}_I^a = \mathrm{diag}[0.5 \quad 0.5 \quad 0.5 \quad 0.2 \quad 0.2 \quad 0.2]$ [1/s], $\boldsymbol{K}_D^a = \mathrm{diag}[0.1 \quad 0.1 \quad 0.1 \quad 0.1 \quad 0.1 \quad 0.1]$ [1/s],
Control parameters of the finger robot: $\boldsymbol{K}_P^f = \mathrm{diag}\left[1.5\times10^4 \quad 1.5\times10^4 \quad 1.5\times10^4\right]$ [Nm/rad], $\boldsymbol{K}_I^f = \mathrm{diag}\left[0.4\times10^3 \quad 0.4\times10^3 \quad 0.4\times10^3\right]$ [Nm/rad], $\boldsymbol{K}_D^f = \mathrm{diag}\left[0.1\times10^3 \quad 0.1\times10^3 \quad 0.1\times10^3\right]$ [Nm/rad],
The total time taken to complete the task is 30 s, Thus, N=6000.

Table 1. Parameters of the experiments using HM.

(A) Tracing a Three Dimensional Sinusoidal Curve

When the amplitude of the desired sinusoidal curve is approximately equal to the total link length of the finger, the manipulability of the finger will fall to a very small value and the tracing task would not be completed without the assist movement of the arm. In this experiment, a three dimensional sinusoidal curve with an amplitude of 0.1[m] is given in Σ_b by

$$\begin{cases} x = 0.709 + 0.1\sin(2\pi k / N) \\ y = 0.079 + 0.3k/(N\sqrt{2}) \\ z = 0.794 - 0.3k/(N\sqrt{2}) \end{cases} \qquad (k = 0,1,2,\cdots,N) \tag{31}$$

where N is the total sampling number.

The obtained positions of the fingertip and the arm's end-effector are shown in Fig.5(a), and the results indicate that the arm also moves along a trajectory similar to that of the given sinusoidal curve to assist the finger to accurately trace the desired curve. The manipulability W_f and magnitude of the arm's velocity $|\dot{\boldsymbol{p}}_t|$ are drawn in Fig.5(b). In this figure, W_f of the finger is higher than W_{fr} during its starting period. Thus, only the finger moves to draw the curve, while the velocity of the arm is almost zero. Once W_f falls below W_{fr}, the velocity $|\dot{\boldsymbol{p}}_t|$ of the arm moves to augment movement of the finger. As a result, the manipulability of the finger increases.

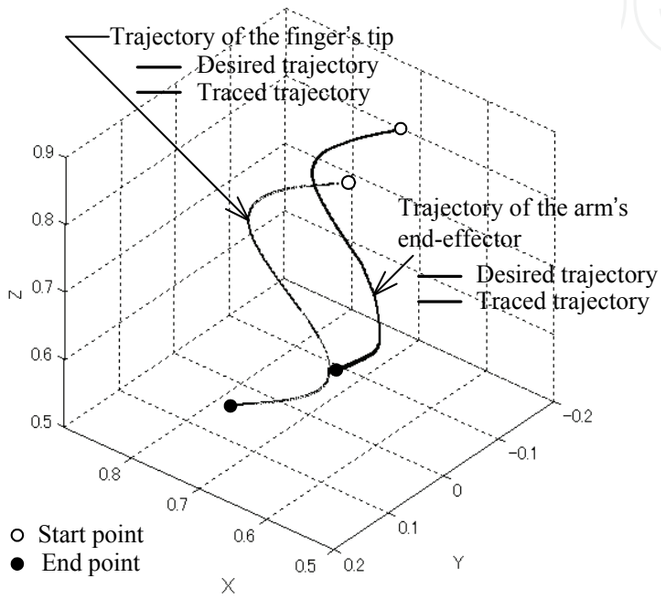

(a) Positions of the arm's end effctor and the fingertip in Σ_b

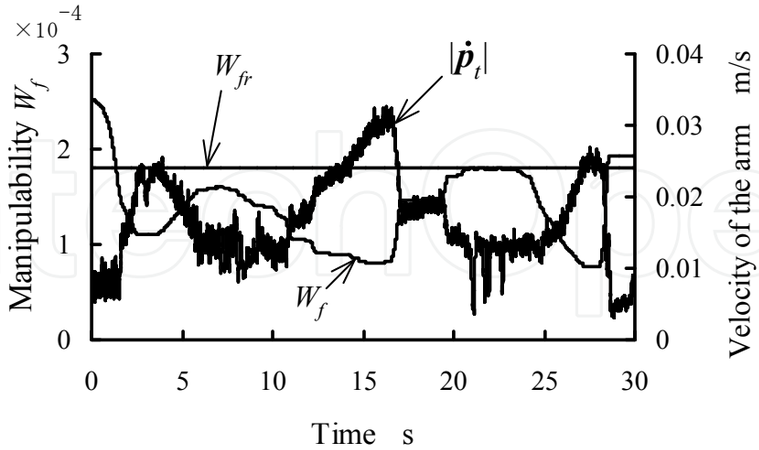

(b) Manipulability of the finger

Fig. 5. Results of tracing a 3D trajectory using the heuristic method

(B) Tracing a Free Hand Figure

The task of tracing a free-hand figure is also completed. This free-hand figure is composed of a small triangle (with edge lengths of 0.03[m], 0.04[m] and 0.05[m]), a small circle (with a

diameter of 0.06[m]) and a longer straight line (with a length of 0.3[m]) to link the circle and the triangle together.

When a human draws such a figure, he will naturally move his finger primarily to draw the delicate part of the figure while he moves his arm to maintain the desired moving potential of his finger. As compared to the arm movement, hand movement consumes less energy because it has a small inertia.

The control parameters used in this experiment are same as listed in Table I, but W_{fr} is set to 0.0002. The positions of the arm's end-effector and the fingertip are shown in Fig.6(a), and the result of W_f is shown in Fig.6(b).

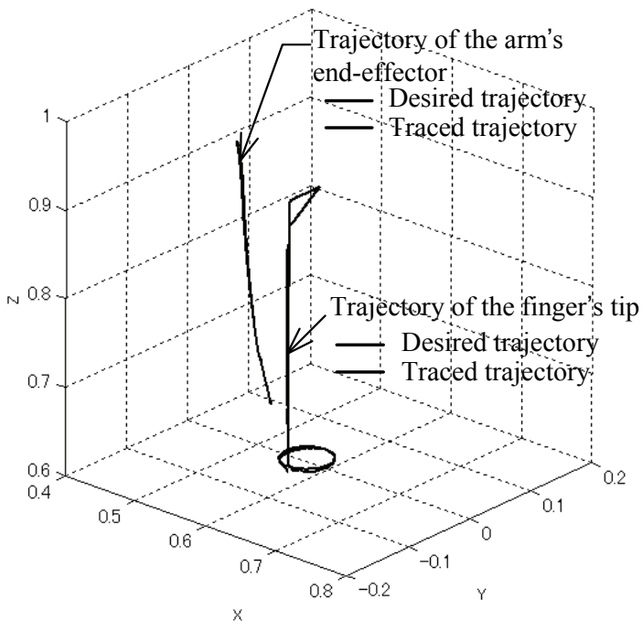

(a) Positions of the arm end effctor and the fingertip in Σ_b

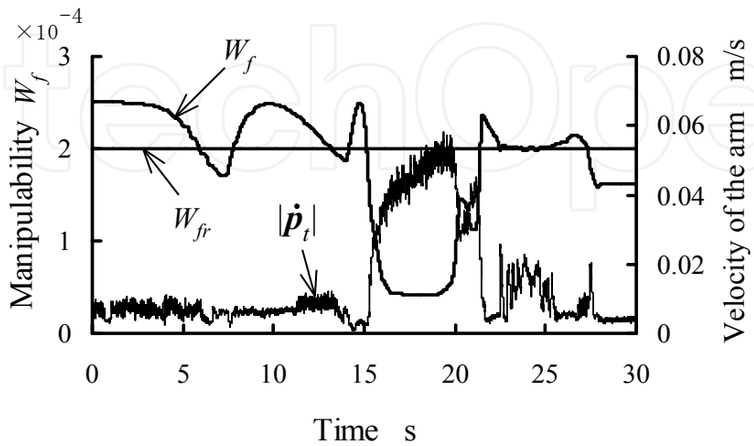

(b) Manipulability of the finger

Fig. 6. Results of tracing a free hand trajectory using the heuristic method

Unlike the movements in experiment I shown in Fig.5(a), the robot finger plays a dominant role in tracing the delicate parts of the triangle and the circle, while the arm moves along the straight line so as to maintain the desired value of the moving potential of the finger. As shown in Fig.6(b), the manipulability W_f of the finger is higher in the initial stages of drawing the triangle. However, the value of W_f falls gradually when the finger begins to move along the straight line toward the circle. To improve the W_f, $|\dot{\boldsymbol{p}}_t|$ of the arm increases resulting in an increase in W_f, as shown in Fig.6(b). When the finger reaches near the position where the circle needs to be traced, the arm stops moving and the finger traces the circle. Thus, the proposed method can naturally segregate the complicated motion of the finger-arm robot into two separate motions of the arm and the finger as in the case of a human being.

4.2 Motion control using SAM

To demonstrate the effectiveness of the steepest ascent method, a few experiments are performed. The control parameters used in the experiments are listed in Table II.

Control sampling interval: T = 0.005 s, Curve width: L = 0.30 [m], A=0.05[m],
Initial position and orientation of the fingertip in Σ_b: x_0 = 0.381 [m], y_0 = 0.025 [m], z_0 = 1.043 [m], a_0 = 0 [rad], β_0 = 1.047 [rad], γ_0 = 0 [rad],
Control parameters of the arm robot: $\boldsymbol{K}_P^a = \mathrm{diag}[8.0 \quad 8.0 \quad 8.0 \quad 24.0 \quad 24.0 \quad 24.0]$ [1/s], $\boldsymbol{K}_I^a = \mathrm{diag}[1.0 \quad 1.0 \quad 1.0 \quad 1.0 \quad 1.0 \quad 1.0]$ [1/s], $\boldsymbol{K}_D^a = \mathrm{diag}[0.01 \quad 0.01 \quad 0.01 \quad 0.01 \quad 0.01 \quad 0.01]$ [1/s],
Control parameters of the finger robot: $\boldsymbol{K}_P^f = \mathrm{diag}[60.0 \quad 60.0 \quad 60.0]$ [Nm/rad], $\boldsymbol{K}_I^f = \mathrm{diag}[0.2 \quad 0.2 \quad 0.2]$ [Nm/rad], $\boldsymbol{K}_D^f = \mathrm{diag}[4.0 \quad 4.0 \quad 4.0]$ [Nm/rad],
Total sampling number: N=6000.

Table 2. Parameters of the experiments using SAM

(A) Tracing a Three Dimensional Sinusoid Curve

For comparing the heuristic method and the steepest ascent method, as shown in Fig.7, experiments are performed for tracing a three dimensional sinusoid curve amplitudes with the fingertip. The sinusoid curve is given as

$$\begin{cases} x = x_0 + Lk/N \\ y = y_0 \qquad\qquad k = 0,1,2,\cdots,N \\ z = z_0 + A\sin(2\pi k/N) \end{cases} \tag{32}$$

where (x_0, y_0, z_0) is the coordinate of the initial position; L, the curve width along the x axis; A, the amplitude of the sinusoid curve; k, the sampling count; and N, the maximum sampling number.

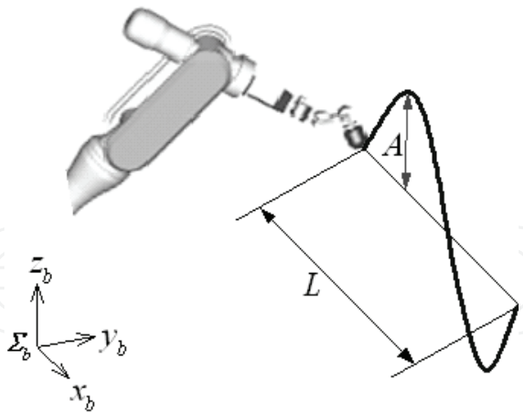

Fig. 7. Tracing a given sinusoid curve with the fingertip

The results obtained from the experiments by applying both the heuristic method and the steepest ascent method to trace the given sinusoid curve are shown in Fig.8(a) and Fig.8(b), respectively. The fingertip position $\boldsymbol{p}_f$ obtained by using both the heuristic method and the steepest ascent method is almost same as the desired $\boldsymbol{p}_{fd}$, as shown in Fig.8(a) and Fig.8(b).

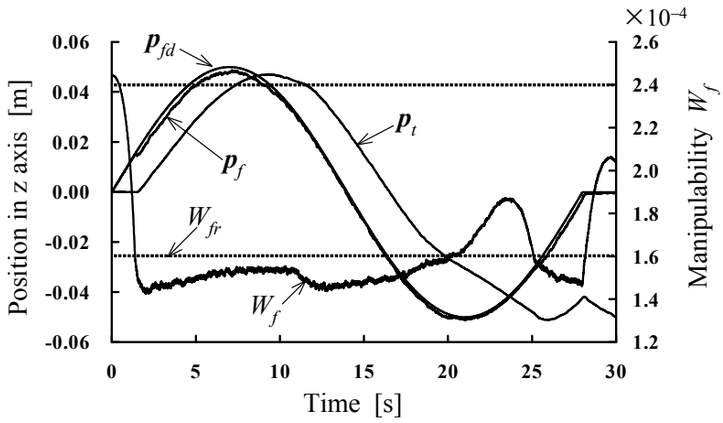

(a) Results obtained by heuristic method (W_{fr} = 1.6×10-4)

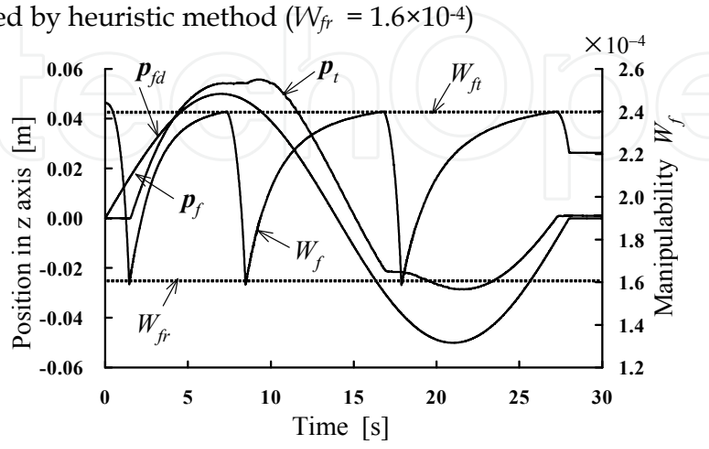

(b) Results obtained by the steepest ascent method (λ=5, W_{fr} =1.6×10-4, W_{ft} =2.4×10-4)

Fig. 8. Results of tracing a sinusoid curve

However, the manipulability W_f of the finger in Fig.8(a), which is obtained by using the heuristic method increases gradually. This is because the basic concept of the heuristic method is to move the arm to a position where the finger's manipulability will not decrease further, instead of directly increasing the manipulability of the finger.

In contrast to the results of the heuristic method, the manipulability W_f of the finger increases significantly and is maintained above W_{fr} for almost the entire duration as indicated by Fig.8(b). This is because, once W_f drops below W_{fr}, the arm moves in the steepest direction which directly provides a moving potential to the finger.

(B) Influence of the Gain Efficient λ

Figure 8(b) indicates that the steepest ascent method effectively modulates W_f above W_{fr} by moving the arm in an efficient manner. In fact, the gain coefficient λ of the steepest ascent method given in (27) determines the speed at which W_f is modulated. To investigate the influence of λ on manipulability regulation, we conduct a few experiments using different values of λ. The results obtained with different values of λ (= 1, 5, and 10) are shown in Fig.9(a), Fig.9(b), and Fig.9(c), respectively.

In all the cases, the arm instantly moves once W_f reduces below W_{fr}. When we set $\lambda = 1$, W_f gradually increases and will finally reach the upper limit W_{ft} as shown in Fig.9(a). However, with a larger value of λ, as shown in Fig.9(b) and Fig.9(c), the arm will generate a fast and strong response for a quick movement. Therefore, W_{fr} increases noticeably and rapidly reaches it upper limit W_{ft}.

5. Discussions

We know that the hand-arm system of a human being has a high redundancy. Even the simplest hand movement requires a series of complicated computations that occur in the CNS. The type of coordinate mapping required and the manner of performing the computations to convert information from exterior space to joint space has perplexed scientists for about half a century. The experimental results of the endpoint stiffness of the human upper limb revealed that the shape and orientation of the stiffness varied proportionally with the location of the hand in the exterior work space (Hogan, et al. 1987). The mechanism of this phenomenon was theoretically summarized and the concept of stiffness ellipsoid was proposed (Mussa-Ivaldi, 1985). Further investigations on hand impedance were also conducted (Tsuji et al. 1988, 1994; Gomi rt al. 1997,1998) and same results revealed that circular ellipsoids are shown almost in front of the body centre, whereas narrow ellipsoids are shown at a greater distance from the body. In fact, the circular shape of the stiffness ellipsoid suggests that the stiffness is uniform in all directions in front of the body centre, whereas the narrow shape of the stiffness ellipsoid represents direction-dependant stiffness present at a greater distance from the body.

In the discussion on the manipulability measure of a robot end-effector, manipulability ellipsoid was first proposed theoretically in a Euclidian space (Yoshikawa, 1985). By using the manipulability theory, we can easily understand why the shape or orientation of the stiffness depends on the hand position. Since a position in front of body centre provides a higher manipulability, locating the hand at that position would provide a higher moving potential in order to easily deal with unexpected situations. Human beings have a natural tendency to move their hands and arms in a position that provides a higher manipulability.

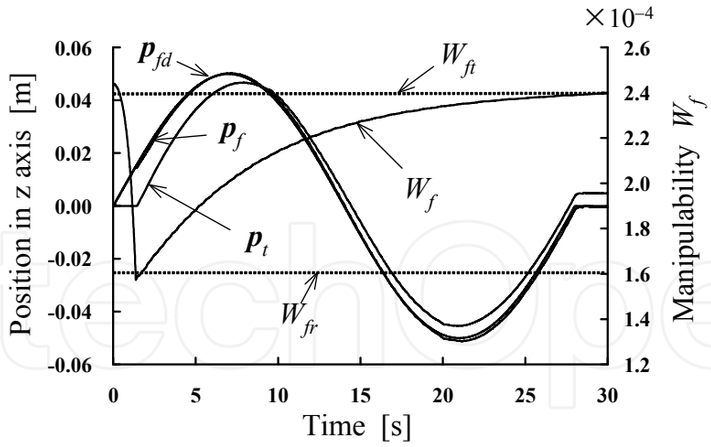

(a) When $\lambda = 1$

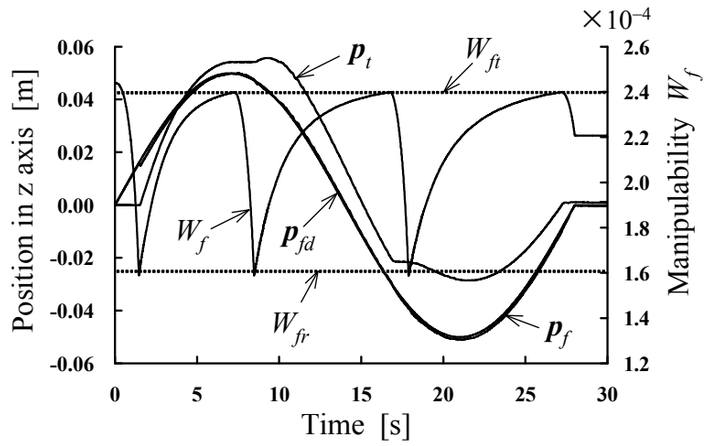

(b) When $\lambda = 5$

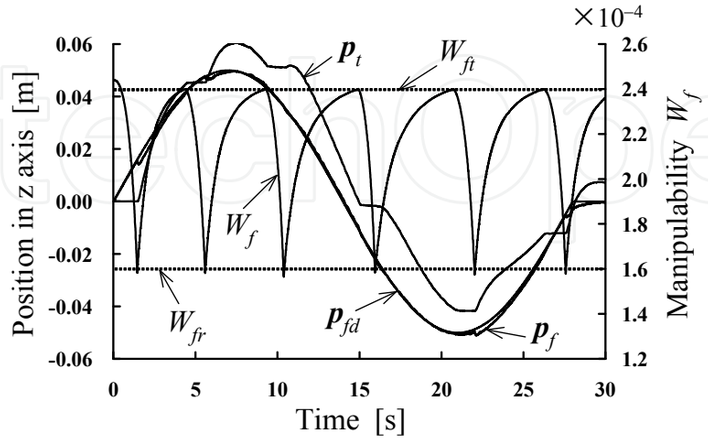

(c) When $\lambda = 10$

Fig. 9. Influence of the gain coefficient on SAM. (W_{fr} = 1.6×10-4, W_{ft} = 2.4×10-4)

This study attempts to propose a motion control for a redundant robot according to the manipulability of the finger inspired by the human hand-arm movement instead of merely calculating a geometric path for determining a kinematics solution.

6. Conclusions

Human beings always adopt the policy of locating their hands in front of the body center. In fact, locating the hand at this position would provide a higher moving potential in order to easily deal with unexpected situations. By using the manipulability theory, we can easily understand this motion policy. As compared to the reported studies, this study attempts to propose a motion control technique for a redundant robot according to its manipulability based on human hand-arm movement instead of merely calculating a geometric path for determining a kinematics solution.

By using the proposed methods of HM and SAM, the finger robot primarily moves, whereas the arm moves only to augment the finger's movement when the finger manipulability reduces below a given reference value. The performance of the finger becomes robust to its singularity by using the proposed steepest ascent method. The experimental results also reveal that the gain coefficient of the SAM plays an important role in response to the change of the finger's manipulability.

7. Future works

In this study, we proposed a motion control to complete unconstrained movement for a finger-arm robot using the manipulability of the finger. A new method of impedance control combined with the proposed method using the manipulability of the finger will be developed for the finger-arm robot to complete a contact task in our future study.

8. References

Furusho, J. & Usui, H. (1989). A control method for manipulator with redundant, *Trans. JSME (C)*, Vol.55, No.514, 1391-1398.

Guo, Z. Y. & Hsia, T. C. (1993). Joint Trajectory Generation for Redundant Robots in an Environment With Obstacles, *J. of Robotics System*, Vol.10(2), 199-215.

Glass, K.; Colbaugh, R.; Lim, D. & Seraji, H. (1995). Real-Time Collision Avoidance for Redundant Manipulators, *IEEE Trans. on Robotics and Automation*, Vol.11(3), 448-457.

Gomi, H & Kawato, M. (1997). Human arm stiffness and equilibrium-point trajectory during multi-joint movement, *Bio. Cybern.*, Vol.76, 163-171.

Gomi, H & Osu, R. (1998). Task dependant viscoelasticity of the human multijoint arm and its spatial characteristics for interaction with environments, *J. of Neuroscience*, Vol.18, 8965-8978.

Hogan, N.; Bizzi, E.; Mussa-Ivaldi, F.A. & Flash, T. (1987). Controlling multijoint motor behavior, *Exerc. Sports Sci. Rev.*, Vol.15, 153-190.

Huang, J.; Quan, B. T.; Harada, M. & Yabuta, T. (2006). Emulating the Motion of a Human Upper Limb: Controlling a Finger-arm Robot by using the Manipulability of its Finger, *Proc. IEEE International Conf. on Robotics and Biomimetics*, 607-612.

Khatib, O., (1986). Real-time obstacle avoidance for manipulators and mobile robots, *Int. J. of Robotics Research*, Vol.5, No.1, 90-98.

Khatib, O. (1995). Inertial Properties in Robotic Manipulation: An Object- Level Framework, *Int. J. of Robotics Research*, Vol.14, No.1, 19-36.

Kim, J. O. & Kholsa, P. K. (1992). Real Time Obstacle Avoidance Using Harmonic Potential Functions, *IEEE Trans. on Robot and Automation*, Vol. 8(3), 338-349.

Loeff, L. A. & Soni, A. H. (1975). An algorithm for computer guidance of a manipulator in between obstacles, *Trans. ASME, J. of Eng. for Industry*, Vol.97, No.3, 836-842.

Ma, S. & Nenchev, D. (1995). Real-time Dynamic Redundancy Control of Redundant Manipulators, *J. of Robotics Society of Japan*, Vol.13(5), 704- 710.

Ma, S.; Hirose, S. & Yoshinada, H. (1996). Efficient Redundancy Control of Redundant Manipulators, *J. of Robotics Society of Japan*, Vol.14(5), 703-709.

Maciejewski, A. A. & Klein, C. A. (1985). Obstacle avoidance for kinematically redundant manipulators in dynamically varying environments, *Int. J. of Robotics Research*, Vol.4, No.3, 109-117.

Melchiorri, C. & Salisbury, J. (1990). Exploiting the Redundancy of A Hand arm Robotic System, *MIT A.I. Memo* No.1261.

Mussa-Ivaldi, F.A.; Hogan, N. & Bizzi, E. (1985). Neural and geometric factors suberving arm posture, *J. Neuroscience*, Vol.5, 2732-2734.

Nagai, K. & Yoshikawa, T. (1994). Impedance control of redundant macro micro manipulator, *J. of Robotics Society of Japan*, Vol.12, No.5, 766-772.

Nagai, K. & Yoshikawa, T. (1995). Grasping and manipulation by robotic arm/ multifingered0hand mechanisms, *JRSJ*, Vol.13, No.7, 994-1005.

Nakamura, Y. & Hanafusa, H. (1986). Inverse kinematics solutions with singularity robustness for robot manipulator control, *Trans. ASME, J. Dyn. Syst., Meas. & Control*, Vol.108, No.4, 163-171.

Quan, B. T.; Huang, J.; Harada, M. & Yabuta, T. (2006). Control of a macro-micro robot system using manipulability of the micro robot, *JSME International Journal (C)*, Vol.49, No.3, 897-904.

Tsuiji, T.; Ito, K.; Nagamachi, M. & Ikemoto, T. (1988). Impedance Regulation in muculo-motor control system and the manipulation ability of the end point, *Trans. SICE*, Vol.24, No.4, 385-392.

Tsuiji, T.; Goto, K.; Ito, K. & Nagamachi, M. (1994). Estimation of human hand impedance during maintenance of posture, *Trans. SICE*, Vol.30, No.3, 319-328.

Vannoy, J. & Xiao, J. (2004). Real-Time Adaptive Trajectory-Optimized Manipulator Motion Planning, *Proc. IEEE/RSJ, Int. Conf. on IROS*, 497-502.

Yoshikawa, T. (1985). Manipulability of robotic mechanisms, *Int. J. of Robotics Research*, Vol.4, No.2, 3-9.

Yoshikawa, T.; Hosoda, K & Doi, T. (1993). Quasi-Static Trajectory Tracking Control of Flexible Manipulator by Macro-Micro Manipulator System, *J. of Robotics Society of Japan*, Vol.11(1), 140-147.

Motion Control

Edited by Federico Casolo

ISBN 978-953-7619-55-8
Hard cover, 590 pages
Publisher InTech
Published online 01, January, 2010
Published in print edition January, 2010

The book reveals many different aspects of motion control and a wide multiplicity of approaches to the problem as well. Despite the number of examples, however, this volume is not meant to be exhaustive: it intends to offer some original insights for all researchers who will hopefully make their experience available for a forthcoming publication on the subject.

How to reference

In order to correctly reference this scholarly work, feel free to copy and paste the following:

Jian Huang, Masayuki Hara, and Tetsuro Yabuta (2010). Controlling a Finger-Arm Robot to Emulate the Motion of the Human Upper Limb by Regulating Finger Manipulability, Motion Control, Federico Casolo (Ed.), ISBN: 978-953-7619-55-8, InTech, Available from: http://www.intechopen.com/books/motion-control/controlling-a-finger-arm-robot-to-emulate-the-motion-of-the-human-upper-limb-by-regulating-finger-ma

INTECH
open science | open minds

InTech Europe
University Campus STeP Ri
Slavka Krautzeka 83/A
51000 Rijeka, Croatia
Phone: +385 (51) 770 447
Fax: +385 (51) 686 166
www.intechopen.com

InTech China
Unit 405, Office Block, Hotel Equatorial Shanghai
No.65, Yan An Road (West), Shanghai, 200040, China
中国上海市延安西路65号上海国际贵都大饭店办公楼405单元
Phone: +86-21-62489820
Fax: +86-21-62489821

IntechOpen